

Triangle diagrams: ternary graphs to display similarity and diversity of earthquake focal mechanisms

Cliff Frohlich

The University of Texas Institute for Geophysics, 8701 N MoPac Exwy, Austin, TX 78759, USA

(Received 22 January 1992, accepted 1 July 1992)

ABSTRACT

Frohlich, C, 1992. Triangle diagrams ternary graphs to display similarity and diversity of earthquake focal mechanisms *Phys Earth Planet Inter*, 75 193–198

This paper presents a new method for displaying focal mechanisms — plotting them on a ternary graph or ‘triangle diagram’ where the vertices represent normal, thrust, and strike-slip focal mechanisms. This method also provides a natural way for determining the relative proportions of thrust, normal, and strike-slip motion for any particular earthquake focal mechanism.

1. Introduction

For regional tectonic analysis, it is often desirable to present information about available earthquake focal mechanisms. The most common and straightforward way to do this is to plot ‘beachballs’ at the epicentral locations on maps, or, if the earthquakes are inconveniently clustered, to display them alongside a map with arrows connecting the beachball and the associated epicenter. Unfortunately, this has limitations because. (1) when the focal mechanisms are not all similar, it is difficult for the eye to pick out individual peculiar mechanisms, or groups of dissimilar mechanisms; (2) nowadays there are more than 9000 focal mechanisms available in the Harvard centroid moment tensor (CMT) file, and thus in large or active regions there are simply too many mechanisms to plot individually.

This paper presents an entirely different method for displaying focal mechanisms — plotting them on a ternary graph or ‘triangle diagram’ where the vertices represent normal, thrust, and

strike-slip focal mechanisms (Fig. 1). An unexpected result is that this method also provides a natural way for determining the proportions of thrust, normal, and strike-slip motion for any particular earthquake focal mechanism. Triangle diagrams were first used to plot earthquake mechanisms by Apperson and Frohlich (1988) and Frohlich and Apperson (1992); however, the present paper presents more complete information about their derivation and use.

2. Triangle diagrams

Triangle diagrams rely on the observation that we can characterize earthquake focal mechanisms as thrust, strike-slip, or normal in terms of the dip angles with respect to horizontal of their T, B, and P axes (Fig. 2). Thus, we say a mechanism is thrust if it possesses a vertical or near-vertical T axis, strike-slip if it has a vertical or near-vertical B axis, and normal if it has a vertical or near-vertical P axis. Moreover, if the P axis is closest to vertical, and the B axis is next closest, we are likely to say that the mechanism is ‘normal with a component of strike-slip.’

Correspondence to C. Frohlich, The University of Texas Institute for Geophysics, 8701 N MoPac Exwy, Austin, TX 78759, USA

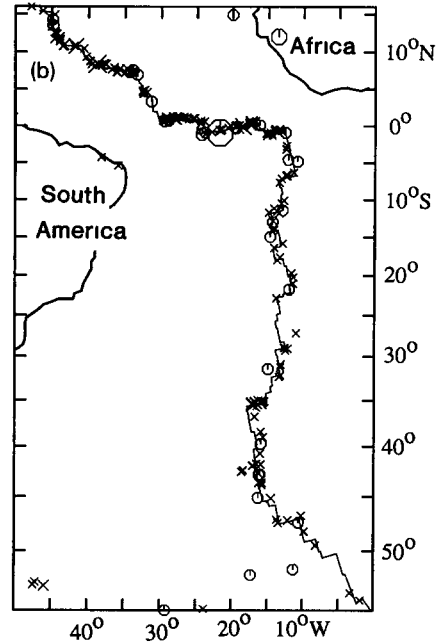
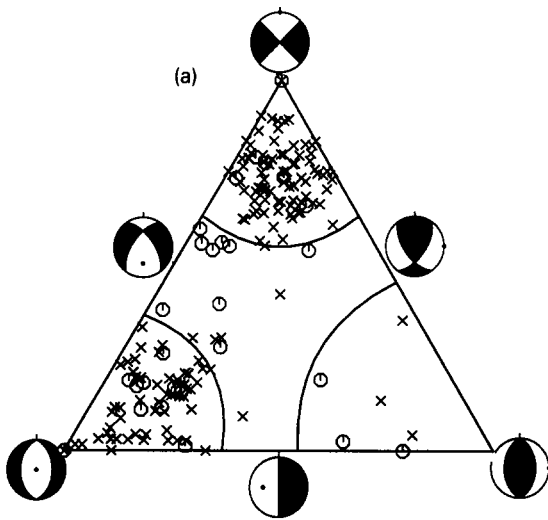


Fig 1 (a) Triangle diagram displaying Harvard CMT mechanisms for earthquakes along the southern Mid-Atlantic Ridge (between 55°S and 16°N, and 50°W and 0°E) The vertices of the triangle represent earthquakes with vertical T axes (thrust mechanisms), vertical B axes (strike-slip), and vertical P axes (normal) X indicates earthquakes with predominantly double-couple mechanisms ($f_{cld} < 0.2$), O indicates earthquakes with mechanisms having a substantial non-double-couple component ($f_{cld} > 0.2$) Note that although mechanisms are concentrated in two clusters near the strike-slip and normal vertices of the triangle, there is considerable variation of mechanism within the clusters Also, even though the southern Mid-Atlantic is a spreading ridge-transform environment, note that there are a few earthquakes with mechanisms closer to the thrust vertex (b) Map showing the location of the ridge-transform boundary is as determined in Royer et al (1992)

Triangle diagrams are simply a quantitative graphical method for using the dip angles of T, B and P axes for displaying focal mechanisms. Al-

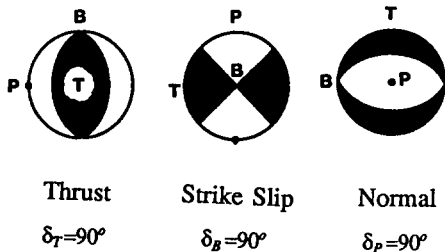


Fig 2 Focal mechanisms are predominantly thrust, strike-slip, or normal, depending on whether their T, B, or P axes are nearest to vertical Thus, if δ_T , δ_B , and δ_P are the dip angles with respect to the horizontal for the T, B, and P axes, we have thrust mechanisms when δ_T is near 90°, strike-slip mechanisms when δ_B is near 90°, and normal mechanisms when δ_P is near 90°

though it is possible to plot mechanisms manually without any quantitative knowledge about them (Fig. 3), usually it is useful to plot them with a computer. It is possible to plot a unique point representing the orientation of the T, B, and P axes because any three mutually perpendicular vectors having dip angles δ_T , δ_B , and δ_P satisfy the identity

$$\sin^2\delta_T + \sin^2\delta_B + \sin^2\delta_P = 1$$

If we define $x = \sin \delta_T$, $y = \sin \delta_B$, and $z = \sin \delta_P$, this identity is just the equation of the sphere $x^2 + y^2 + z^2 = 1$. Since all the angles are between 0 and 90°, plotting focal mechanisms on the triangle diagram is equivalent to the cartographer's problem of projecting locations from a quarter-hemisphere onto a triangular flat surface.

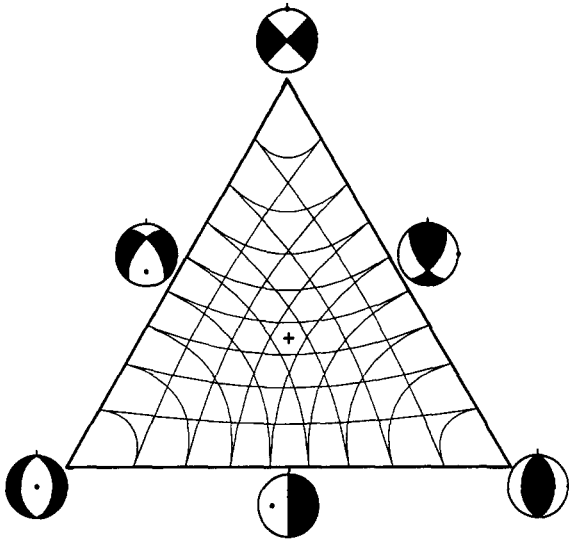


Fig 3 Triangle diagram suitable for plotting focal mechanisms manually, given dip angles δ_T , δ_B , and δ_P for T, B, and P axes. At the vertices of the triangle the dip angles are 90° , and the curved lines delineate where the dip angles are 80° , 70° , 60° , 50° , 40° , 30° , 20° , and 10° . The + in center marks the mechanism where $\delta_T = \delta_B = \delta_P = 35.26^\circ$.

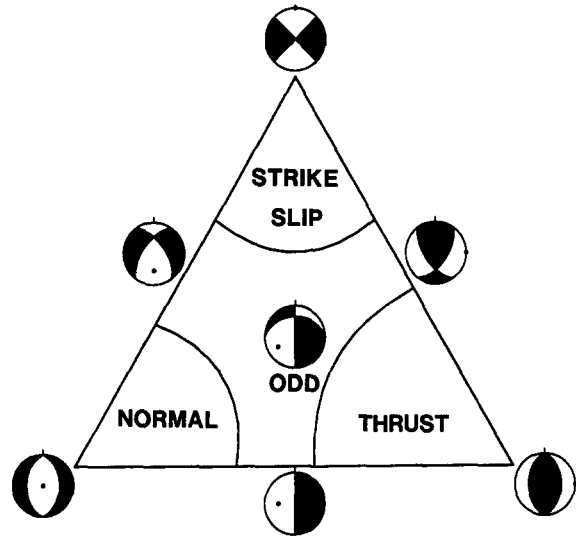


Fig 4 Definition of focal mechanism categories for shallow earthquakes. Analysis of Harvard CMT for earthquakes with depths less than 50 km suggests that we define strike-slip and normal mechanisms as those having B and T dip angles δ_B and δ_T , greater than 60° , and thrust earthquakes as those having δ_P greater than 50° . We define mechanisms satisfying none of these criteria to be 'odd' mechanisms. This figure is reproduced from Frohlich and Apperson (1992).

The map projection which does this is the azimuthal gnomonic projection (Richardus and Adler, 1972). If Ψ is the angle defined by

$$\Psi = \tan^{-1}(\sin \delta_T / \sin \delta_P) - 45^\circ$$

then the horizontal position h and vertical position ν of a point on the triangle diagram are given by

$$h = \frac{\cos \delta_B \sin \psi}{\sin(35.26^\circ) \sin \delta_B + \cos(35.26^\circ) \sin \delta_B \cos \psi}$$

$$\nu = \frac{\cos(35.26^\circ) \sin \delta_B - \sin(35.26^\circ) \cos \delta_B \cos \psi}{\sin(35.26^\circ) \sin \delta_B + \cos(35.26^\circ) \sin \delta_B \cos \psi}$$

Here, 35.26° is the dip angle of the T, B, and P axes for the focal mechanism which plots in the exact center of the triangle diagram, where $h = \nu = 0$.

3. Partitioning of normal, strike-slip and thrust

Because the sum of squares of the sines of dip angles for T, B, and P axes equals unity, for any focal mechanism it is convenient to define the relative proportions f_{thrust} , $f_{strike-slip}$ and f_{normal} :

$$f_{thrust} = \sin^2 \delta_T$$

$$f_{strike-slip} = \sin^2 \delta_B$$

$$f_{normal} = \sin^2 \delta_P$$

Thus, for example, when the B axis is vertical $f_{strike-slip} = 1$, and f_{normal} and f_{thrust} are zero. However, for a mechanism where all three dip angles are the same, equaling 35.26° , then $f_{strike-slip} = f_{normal} = f_{thrust} = 0.33$.

Frohlich and Apperson (1992) used this scheme to characterize earthquake mechanisms as thrust, strike-slip, normal, and 'odd' (Fig 4). Their analysis of earthquake mechanisms at 'typical' plate boundaries suggested defining strike-slip and normal mechanisms as those with the B axis or P axis within 30° of the vertical ($f_{strike-slip}$ or $f_{normal} > 0.75$), and thrust mechanisms as those with T axes within 40° of the vertical ($f_{thrust} > 0.59$). They defined all other mechanisms as 'odd'.

The characterization of earthquake mechanisms as thrust, normal, and strike-slip has physi-

cal significance since the distribution of orientations of real earthquake mechanisms is clearly not random. As explained by Frohlich and Wille-

mann (1987), the proportion of a focal sphere within an angle θ of any axis equals $(1 - \cos \theta)$. Thus, for randomly oriented mechanisms a frac-

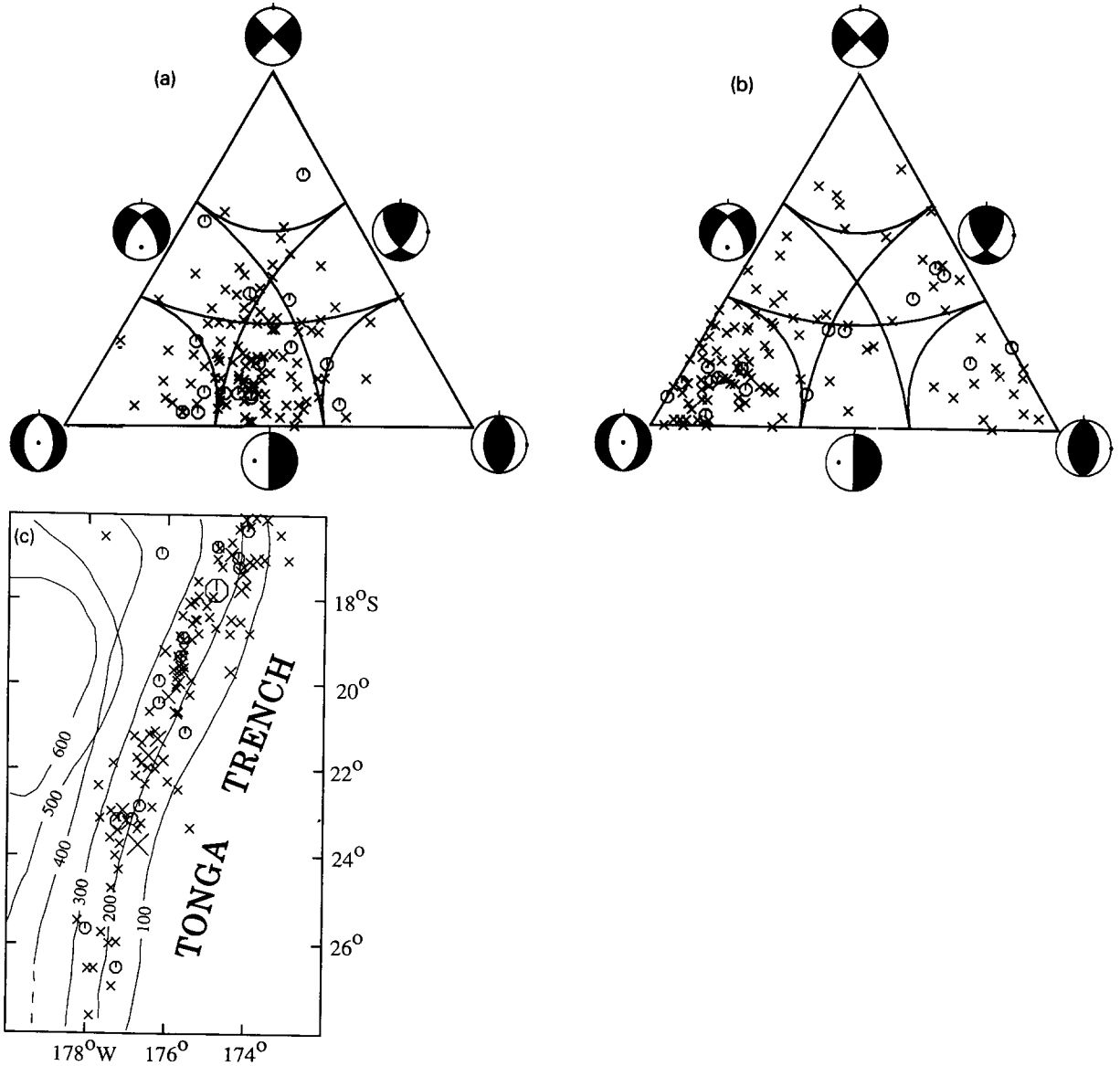


Fig 5 Triangle diagrams displaying mechanisms for intermediate depth earthquakes from the Tonga-Kermadec region ($100 \text{ km} < h < 300 \text{ km}$, epicenters between 16°S and 28°S , and 175°E and 170°W) (a) Mechanisms in ordinary map coordinates (b) Mechanisms presented in a coordinate system where the Tonga-Kermadec slab is approximately vertical, i.e. the mechanisms are rotated 20° about the vertical axis and then 35° about the north axis Symbols are as in Fig 1 (c) Map showing location of earthquakes plotted in (a) (b) Symbols are as in Fig 1 The contour lines represent the approximate depth of the Wadati-Benioff zone as determined by Burbach and Frohlich (1986)

TABLE 1

Observed incidence of thrust, strike-slip, normal, and 'odd' earthquakes in the Harvard CMT catalog, and incidence expected if earthquake mechanisms were oriented randomly in space

Type	Number	Fraction	
		CMT	Random
Thrust	2503	0.474	0.234
Strike-slip	1271	0.241	0.134
Normal	816	0.154	0.134
Odd	686	0.131	0.498
Total	5276	1.000	1.000

Table includes only earthquakes with focal depths $h < 50$ km, and $f_{\text{cld}} < 0.2$. Here f_{cld} is the ratio of the principal moments of largest and smallest absolute value — f_{cld} is zero for double-couple earthquake mechanisms, and is 0.5 for a pure compensated linear vector dipole mechanism

tion 0.134 will be normal (P within 30° of the vertical axis), 0.134 will be strike-slip, and 0.234 will be thrust (T within 40° of vertical). In the Harvard CMT catalog, shallow earthquakes having predominantly double-couple mechanisms ($h < 50$ km, $f_{\text{cld}} < 0.20$) are about twice as likely to have thrust or strike-slip mechanisms than randomly oriented mechanisms (Table 1). However, although we would expect about half of all random mechanisms to be 'odd,' real earthquakes have odd mechanisms only 13% of the time.

4. Two examples

The southern part of the Mid-Atlantic Ridge is a classic spreading ridge–transform environment where earthquakes mechanisms tend to cluster near either the normal or strike-slip vertices of the triangle diagram (Fig. 1). The diagram shows clearly that all but a handful of focal mechanisms either have P or B axes oriented within 30° of the vertical, however, a substantial number do have axes more than 20° from the vertical. A few earthquakes do lie outside the normal and strike-slip regions, however, the majority of these have non-double-couple mechanisms.

Triangle diagrams can also be a useful method for displaying the variability in intermediate and

deep earthquake mechanism. For example, between 100 and 300 km depth the Tonga–Kermadec Wadati–Benioff zone is regular and generally planar, with a dip of about 55° . Moreover, although earthquake mechanisms are decidedly non-random (Fig. 5(a)) they also are much less clustered than are those in Fig. 1. In a rotated coordinate system where the Wadati–Benioff zone is vertical (Fig. 5(b)) the mechanisms are predominantly down-dip tensional. However, a significant number of mechanisms exhibit down-dip compression, and a few have down-dipping B axes or odd mechanisms. As noted by Apperson and Frohlich (1987), this scatter is typical for mechanisms or earthquakes in Wadati–Benioff zones. A point plotted on a triangle diagram depends only on the dip angles of the T, B, and P axes, and not on the azimuthal orientation of the earthquake mechanism. Thus triangle diagrams are especially useful for evaluating diversity of mechanisms in arc-shaped subduction zones, as long as the dip of the Wadati–Benioff zone is approximately constant.

Acknowledgments

The author thanks Roberto Gutierrez and K. Denise Apperson for initially suggesting ternary diagrams as a means to display earthquake sources. We thank our colleagues at Harvard University for sending us centroid moment tensor information. The National Science Foundation provided support for this research under grants EAR-8916665 and EAR-9105069.

References

- Apperson, K.D. and Frohlich, C., 1987. The relationship between Wadati–Benioff zone geometry and P, T and B axes of intermediate and deep focus earthquakes. *J. Geophys. Res.*, 92, 13821–13831.
- Apperson, K.D. and Frohlich, C., 1988. Sums of moment tensors for earthquakes near subduction zones. *EOS, Trans. Am. Geophys. Union*, 69, 1438.
- Burbach, G.V. and Frohlich, C., 1986. Intermediate and deep seismicity and lateral structure of subducted lithosphere in the Circum-Pacific region. *Rev. Geophys.*, 24, 833–874.

- Frohlich, C and Apperson, K D , 1992 Earthquake focal mechanisms, moment tensors, and the consistency of seismic activity near plate boundaries *Tectonics*, 11 279–296
- Frohlich, C and Willemann, R J , 1987 Statistical methods for comparing directions to the orientations of focal mechanisms and Wadati–Benioff zones *Bull Seismol Soc Am* , 77 2135–2142
- Richardus, P and Adler, R K , 1972 *Map Projections North Holland, Amsterdam*, 174 pp
- Royer, J Y , Muller, R D , Gahagan, L M , Lawver, L A , Mayes, C L , Nurnberg, D and Sclater, J G , 1992 *A Global Isochron Chart The University of Texas Institute for Geophysics, Tech Rep No 117, Austin, TX*, 25 pp